Alluvial Architecture of the Early Pennsylvanian Sharon Formation in Northeastern Ohio[1]

DAVID J. NINKE AND JAMES E. EVANS, BP Exploration (Alaska), Inc., P.O. Box 196612, 900 East Benson Blvd., Anchorage, AK 99519 and Department of Geology, Bowling Green State University, Bowling Green, OH 43403

ABSTRACT. In northeastern Ohio, excellent exposures of the Sharon Formation allow study of the architecture (3-D geometry) of these gravel- and sand-bedload stream deposits. Specific architectural elements include gravel bar-platform deposits (including bar head, bar core, and bar tail sub-elements), suprabar-platform deposits (laminated sand sheets and chute channel-fills), bar-margin foreset deposits, and sandy 2-D and 3-D dune deposits. Paleochannels had a depth-to-width ratio of 1:10 (r^2 = 0.69) for gravel-bedload streams and 1:40 (r^2 = 0.89) for sand-bedload streams. Channel paleoslopes were between 0.3 to 1.1 m/km and transported clasts with D_{95} = 5.6 cm. These data are consistent with modern, braided streams.

In this region, Late Mississippian to Early Pennsylvanian glacio-eustatic baselevel fall resulted in subaerial erosion of the underlying marine shales and formation of paleovalleys. Subsequent baselevel rise created accommodation space that was filled by deposition of the Sharon Formation in two separate phases: (1) backfilling of paleovalleys and (2) unconfined fluvial depositional systems after the paleovalleys were filled and overtopped. The transition of fluvial systems from confined to unconfined probably resulted in braidplain widening and changes in bank materials, explaining observed changes in paleohydraulics and fluvial sedimentology of the unit.

OHIO J SCI 102 (4):70–81, 2002

INTRODUCTION

Continental depositional systems evolve in response to changes in eustasy, tectonics, sediment supply, and paleoclimate (Zeuner 1959; Butcher 1990; Evans and Terry 1994). The Early Pennsylvanian Sharon Formation of northeastern Ohio illustrates a complex response to Carboniferous glacio-eustasy and foreland basin subsidence, during an interval of progressive climate change. The purpose of this research is to interpret the depositional environment of the Sharon Formation (using facies analysis, paleohydraulic analysis, and alluvial architectural analysis), and to evaluate the relative importance of external controlling variables (for example, tectonics, eustasy, and paleoclimate) versus internal hydrological processes (for example, changes in lateral migration rates, channel morphology, and bank materials) on the unit's history.

Geologic Background

During the Pennsylvanian Period (320-286 Ma), the collision of North America and Africa resulted in the Alleghenian Orogeny and final assemblage of Pangaea. Along its western boundary, thin-skinned deformation created the Appalachian Mountains as a fold-and-thrust belt with an associated foreland basin (Hatcher 1972; Allmendinger and others 1987). The Appalachian foreland basin, found west of the deformed upper plate, was at least 225 km wide and 650 km long, and extended SW-NE through the field area in northeastern Ohio.

Sediments of the Early Pennsylvanian Pottsville Group (including the Sharon Formation) were shed into the Appalachian foreland basin from the advancing thrust sheets to the east, and also from a landmass in Ontario and Quebec (for example, Meckel 1967; Krissek and others 1986). This northern landmass has been interpreted as evidence of a peripheral bulge that formed west of the foreland basin due to isostatic effects (Slingerland and Beaumont 1989). Previous workers have suggested that fairly subtle changes in sedimentation of the Pottsville Group can be attributed to the interplay of thrust advancing and resulting isostatic adjustments of the foreland basin and of the peripheral bulge (for example, Robinson and Prave 1995).

Mississippian and Pennsylvanian times were also affected by continental glaciation, glacio-eustatic sea-level changes, and changes in paleoclimate. Evidence suggests these glaciations were periodic on Milankovitch time-scales (100 and 400 k.y.) due to astronomical forcing (Crowell 1978; Algeo and Wilkinson 1988; Gastaldo and others 1996). Consequences of the repeated growth or recession of continental glaciers were glacio-eustatic changes in sealevel and repeated sequences of sediments (called "cyclothems") which formed due to shifting positions of shorelines (Wanless and Shepard 1936; Crowell 1978; Ross and Ross 1985). Cyclothems were globally widespread during the Pennsylvanian (Veevers and Powell 1987) and are evident in upper portions of the Pottsville Group (Algeo and Wilkinson 1988), but are rare in southeastern Ohio (Nadon 1998), and are entirely lacking in the Sharon Formation.

Mississippian and Pennsylvanian strata from the Appalachian foreland basin also document progressive changes from arid to humid conditions. Late Mississippian rocks in this region consist of marine carbonates, shales, evaporites, eolianites, continental redbeds, and certain characteristic paleosols (for example, calcareous aridisols and vertisols), which show that this portion of the Appalachian foreland basin was located in the arid

[1]Manuscript received 2 June 2000 and in revised form 15 January 2002 (#00-10).

subtropics (Cecil 1990; Cecil and others 1997; Miller and Eriksson 1999). Recent studies have shown increasing paleoclimatic variability (wet-dry cycles) that operated at Milankovitch frequencies approaching the Mississippian-Pennsylvanian transition (Miller and Eriksson 1999). The overlying Lower Pennsylvanian rocks consist of quartz sandstones, aluminum-rich clays, and thick coals, which indicate more humid conditions (Phillips and Peppers 1984; Cecil 1990; Miller and Eriksson 1999). Recent studies suggest that, during Early to early Middle Pennsylvanian, paleoclimate fluctuated from ever-wet conditions during sea level low stands, to wet but seasonally dry conditions during high stands (Cecil and Dulong 1998).

Sharon Formation

The Sharon Formation is the basal unit of the Early Pennsylvanian Pottsville Group. There are two very different outcrop areas. The Pottsville Group of eastern Pennsylvania is wedge-shaped (300 m thick on the east and thinning westward), and consists of fluvial deposits with westerly paleocurrents (Meckel 1967; Robinson and Prave 1995). In contrast, the Pottsville Group of northeast Ohio and western Pennsylvania is sheetlike, considerably thinner, and has southerly paleocurrents (Meckel 1967; Collins 1979).

In Ohio and western Pennsylvania, the local thickness of the Sharon Formation varies considerably. Where erosional paleovalleys were cut into the underlying Mississippian Cuyahoga Group, the Sharon Formation reaches a maximum thickness of about 80 m (Coogan and others 1974; Krissek and others 1986), while elsewhere the unit averages 15 m thick (Winslow and White 1966). Most of the Sharon Formation consists of conglomerate and sandstone, but a shale-rich, thin, upper unit ("Sharon Shale Member" of Meckel 1967) has also been recognized. In northeastern Ohio, the conglomerates occupy N-S oriented narrow belts where the percent conglomerate and grain size decreases to the south (Lamb 1911; Fuller 1955; Meckel 1967). Clasts are spherical and well rounded, with a maximum diameter of 17 cm. Conglomerates consist of vein quartz, quartzite, sandstone, slate, shale, silicified Devonian limestone, and rare plutonic or high-grade metamorphic clasts (Meckel 1967).

Paleogeographical reconstructions indicate that the closest marine units of equivalent age were located 160-200 km south of the study area, and that the closest sediment source areas were located between 80-120 km (sedimentary rock fragments) and 290-320 km (igneous and metamorphic rock fragments) to the northeast (Meckel 1967). The trend of gravel-rich deposits, paleocurrents, and the locations of source areas and marine units are consistent with south-flowing fluvial systems (Meckel 1967).

There have been a variety of depositional interpretations for the Sharon Formation. The earliest workers interpreted the unit as marine (Butts 1908; Stout 1916). Then for a period of time it was popular to interpret the unit as alluvial fan (Fettke 1938; Bowen 1953; Fuller 1955) or deltaic (Lamb 1911; Bowen 1953; Fuller 1955). Most recent workers agree the unit represents some type of fluvial depositional environment, such as "fluvial sheet gravels" (Meckel 1967), meandering stream systems (Mrakovich 1969) or braided stream systems (Mrakovich 1969; Mrakovich and Coogan 1974; Krissek and others 1986; Wells and others 1993). The evidence typically cited in support of a braided stream model includes prevalence of massive or planar-bedded conglomerate and cross-bedded sandstone, low paleocurrent dispersion, and lack of characteristic vertical sequences such as point-bar sequences seen in meandering streams. This paper shall employ several additional tools, such as Markov Chain analysis, fluvial depositional architecture, and paleohydraulics to evaluate these earlier interpretations.

MATERIALS AND METHODS

Field Work

Stratigraphic sections were measured at four localities (Figs. 1,2). Individual beds in each section were classified using a lithofacies code (Table 1). Each section was incorporated into photomosaics that emphasized viewing deposits in three-dimensions wherever possible. Many of the outcrops are jointed, permitting viewing of intersecting two-dimensional rock faces (Fig. 3). Other field data includes sedimentary structures, paleocurrent measurements, and detailed grain-size measurements from certain beds. Paleocurrent data was analyzed using the program ASTRA.BAS (Wells 1999).

Markov Chain Analysis

Each stratigraphic section was evaluated using Markov chain analysis, which tests whether or not the succession of bedding has a random order. If the transition from one lithofacies to another fails the Chi-square test, then the transition is non-random and is investigated for

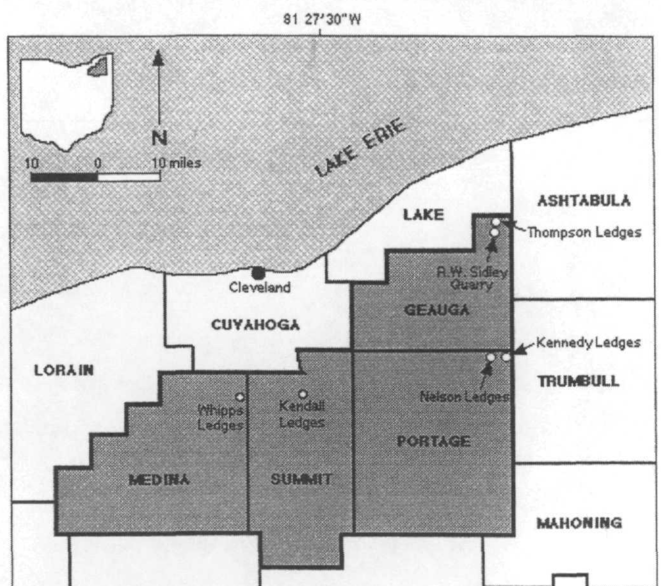

FIGURE 1. Map showing the location of outcrops of the Sharon Formation in northeastern Ohio.

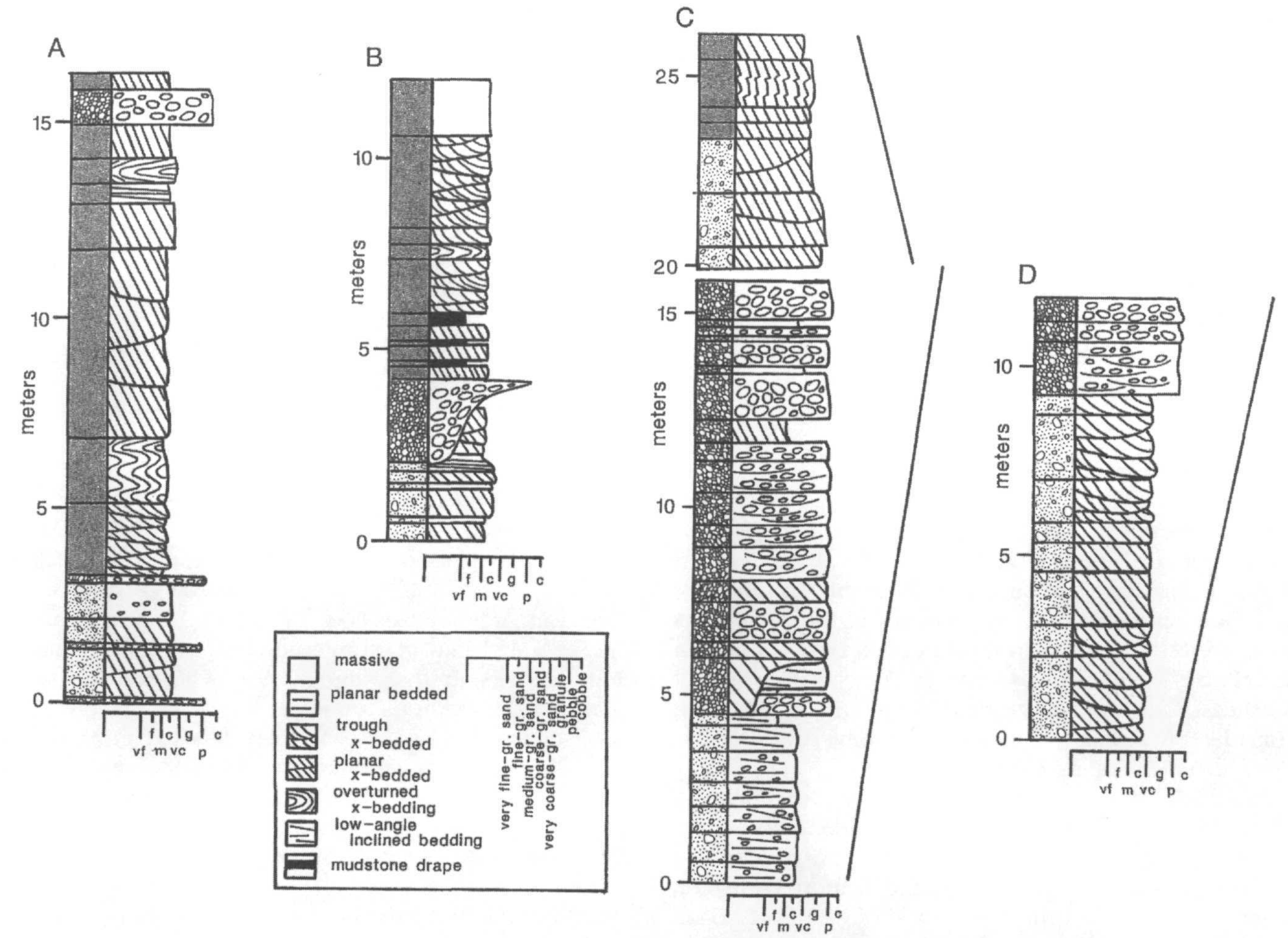

FIGURE 2. Stratigraphic sections measured at: A) Whipps Ledges, B) Kendall Ledges, C) Kennedy-Nelson Ledges, and D) Thompson Ledges.

TABLE 1

Lithofacies in the Sharon Formation.

Lithofacies Code	Lithology	Sedimentary Structures	Environmental Interpretation
Gm	conglomerate	massive, imbrication	bar-head or bar-core
Gh	conglomerate	stratified, inclined <10^{0}	bar-tail
Gp	conglomerate	planar-tabular crossbeds	bar-margin foresets
Smc	sandstone	massive	bar-top deposit
Sh	sandstone	stratified	bar-top deposit
Sp	sandstone	planar-tabular crossbeds	2-D dune deposit
St	sandstone	trough crossbeds	3-D dune deposit
Sr	sandstone	ripple laminated	ripples
Se	sandstone with mud intraclasts	massive	scour fills
Ss	pebbly sandstone	scours	scour fills
Fm	siltstone	massive	mudstone drapes

Modified from Miall 1977, 1978; Rust 1978.

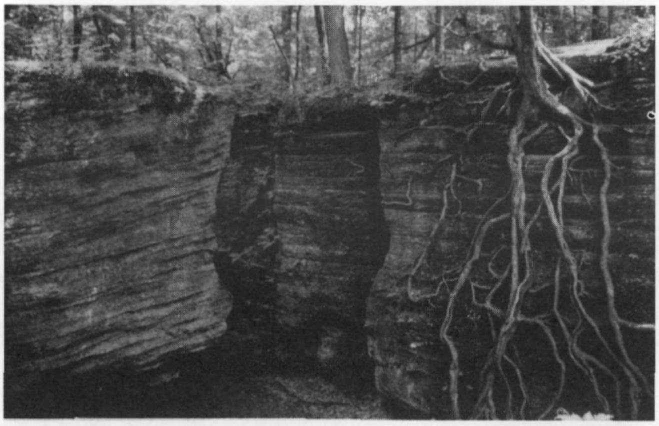

FIGURE 3. Photograph of field sites showing the weathering-enhanced joint pattern which makes possible three-dimensional views of fluvial deposits in the Sharon Formation.

underlying geological causes. The lithofacies transition matrices are given in Ninke (1995). The statistical tests were performed from Biomedical Display Package (BMDP) 4F (Brown 1983), using the iterative, proportional fitting method to obtain expected cell counts in a matrix of random expectations (Turk 1979; Powers and Easterling 1982). Non-random transitions were identified through analysis of residuals that have been converted to normalized variables and tested at the 95% significance level (Powers and Easterling 1982). The problem of masking of outliers (for example, Harper 1984) has been resolved using a multistep procedure that tests the matrix, removes the cell causing largest deviation from quasi-independence, then retests the matrix for other cells (Carr 1982).

Paleohydraulic Analysis

Reconstructing the flow conditions that resulted in the deposits of the Sharon Formation was accomplished by determining the dimensions of channels, the grain sizes transported by the streams, and the paleoslopes. Bankfull channel depth was obtained from the depth of scours, the maximum relief of gravel bar platforms, the maximum relief of bar-margin avalanche faces, and the height of dunes (Boothroyd and Ashley 1975; Ethridge and Schumm 1978; Friend 1978; Evans 1991; Mohrig and Smith 1991). Bankfull channel width was obtained by measurements from photomosaics.

Two separate grain size measurements were conducted in the field, D_{95} and D_{50}. D_{95} measures the largest size of clasts moving through the channel. Accepted practice for obtaining D_{95} is to measure the intermediate grain diameter of the ten largest clasts found at the base of each individual bed (Maizels 1983; Evans 1991). D_{50} represents the median of the grain size distribution. It can be obtained directly from the range of the intermediate clast diameter found at the base of each individual bed.

Paleoslope is obtained by simplifying the equations governing fluid flow to the case of a steady, horizontally uniform flow in a natural channel, where friction on the walls of the channel is negligible compared to that on the channel bottom. Under these conditions, the boundary shear stress acting on the bed of the channel can be calculated as:

$$\tau_b = \rho g h S$$

where τ_b = the boundary shear stress
ρ = the fluid density
g = the acceleration due to gravity
h = the flow depth
and S = the slope of the water surface

Both field and laboratory experiments have shown that initial motion of bed materials in coarse-grained rivers typically occurs at a transport stage (for example, a ratio of (τ_{cr}) maximum to (τ_b) general motion) of between 1 and 3 (Andrews 1983, 1984).

The critical shear stress (τ_{cr}) represents the necessary boundary shear stress to move the bedload materials, based upon their grain size, grain shape, sorting, effective density, and roughness. The values can be obtained from the Shields relationship:

$$\tau_{cr} = (\tau^*)_{cr}(\rho_s - \rho)gD$$

where τ_{cr} = the critical shear stress
$(\tau^*)_{cr}$ = the non-dimensional critical shear stress ("Shields Number")
ρ_s = the grain density (assumed to be quartz, with a density of 2.65 g/cm^3)
ρ = the fluid density
g = the acceleration due to gravity
D = the nominal grain diameter

This paper uses the method of Wiberg and Smith (1987) to obtain the Shields Number from an evaluation of grain protrusion and the particle angle of repose, as obtained by the ratio of the grain size of interest (D_{95}) and the local bed roughness, as indicated by the median grain size (D_{50}). Paleoslopes were calculated from solving these equations for slope when the transport stage was set to 1 (initial motion), using paleohydraulic data for bankfull depth, and grain size data (Mohrig 1987; Evans 1991).

Alluvial Architecture

The method of applying photomosaics and numerous, closely spaced stratigraphic sections to determine the three-dimensional geometry of fluvial deposits was developed elsewhere (Allen 1978; Bluck 1979; Bridge and Leeder 1979; Friend 1983; Miall 1985, 1993, 1994). This study applies the terminology of Miall (1985) to the genetic interpretation of alluvial architecture (Table 2). Each architectural element consists of one or several lithofacies that are separated vertically and laterally from other architectural elements by bounding surfaces that, in sum, delineate the three-dimensional shape of the deposit. Bounding surfaces and the architectural units they delineate can be interpreted by comparison to similar features in modern streams and related environments (Miall 1993, 1994).

RESULTS

Lithofacies Analysis

Representative stratigraphic sections are shown in Fig. 2. Eleven lithofacies were identified in the Sharon Formation (Table 1). Complete description and

TABLE 2

Architectural elements in the Sharon Formation.

Element	Code	Typical Lithofacies	Geometry & Relationships
Channel-fill Deposits			
Major channels	CH	any combination	broadly lenticular
Chute Channels	CHc	Sp, St, Sr, Fm	lenticular
Bar-Platform Deposits			
Bar-head deposit	GBh	Gm	tabular
Bar-core deposit	GBc	Gm	tabular
Bar-tail deposits	GBt	Gm, Gh	tabular
Bar-margin Foreset deposits	GBf	Gp	wedge shaped
Sandy Bedforms	SB	Sp, St	tabular & wedge shaped
Supra-bar Platform Deposits			
Bar-top deposits	SP	Smc, Sh, Sr	tabular
Chute channels-fills	CHc	Sp, St, Sr, Fm	lenticular

Modified from Miall (1985). Note that "Foreset macroforms" of Miall (1985) are incorporated into Bar-platform deposits as element GBf.

interpretation of each lithofacies is given elsewhere (Ninke 1995). Deposits in the Sharon Formation fall into two general categories: gravel-dominant (mostly lithofacies Gm, Gh, Gp, and Sp) or sand-dominant (most lithofacies St and Sp).

Massive to crudely stratified conglomerates (lithofacies Gm) are found in sheets between 12 cm and 155 cm thick (average 75 cm thick). Each sheet consists of clast-supported, pebble-cobble conglomerate, with an infiltrated matrix of medium- to coarse-grained sandstone. Clasts are spherical, which may explain the rarity of imbrication. By analogy to modern deposits, lithofacies Gm represents the bar head or bar core portion of a bar platform, in a gravel-bedload stream (Rust 1978; Miall 1978; Bluck 1979). The lower contact is typically a scoured surface (lithofacies Ss). The bar core can be overlain by massive or stratified sandstone (lithofacies Smc or Sh), displaying primary current lineation, indicative of high flow rates. These deposits represent suprabar-platform deposits (Fig. 4) that form during high flow stage, when the bar platform is entirely submerged. Alternatively, the bar platform can be incised by small channels that were infilled with cross-bedded (lithofacies St) or ripple-laminated sandstone (lithofacies Sr). These deposits represent small chute channels which were cut during falling stage, and later filled by small bedforms (for example, Bluck 1979).

In the downstream direction, the massive pebble-cobble conglomerates (lithofacies Gm) are laterally transitional to stratified pebble conglomerates (lithofacies Gh). These deposits consist of beds averaging 49 cm thick that are gently dipping (<10^0) downstream

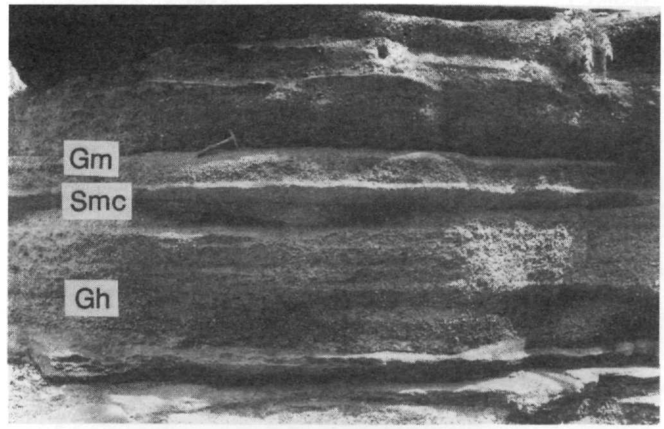

FIGURE 4. Longitudinal (downstream) view of multiple sequences of interbedded gravel bar-core deposits (lithofacies Gm and Gh) with suprabar platform deposits (lithofacies Smc and Sh). Hammer (30 cm) for scale.

(Figs. 5,6). Downstream fining of grain size can be observed. In modern rivers, these deposits represent the bar tail region, which grows by accretion of fine-grained gravel in the lee of the bar head and bar core region (Bluck 1979).

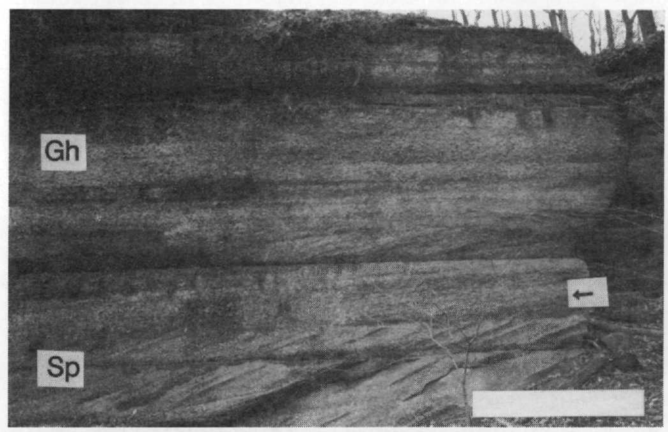

FIGURE 5. Longitudinal (downstream) view of multiple sequences of gravel bar-tail deposits (lithofacies Gh) and sandy bedforms (lithofacies Sp). Arrow indicates gently downstream-dipping bar-tail deposits. Scale bar is 50 cm.

Deposits found adjacent to the bar-platform include planar-tabular cross-bedded conglomerate (lithofacies Gp). These deposits are typically wedge-shaped, with non-erosional bases (Figs. 7,8), and are characterized by normal grading within the foreset laminae. Similar features in modern gravel-bedload streams are bar-margin foreset deposits. These deposits form where a chute channel crosses a gravel bar and forms a set of prograding foresets in the downstream pool (Bluck 1979).

Planar-tabular cross-bedded sandstone (lithofacies Sp) is interstratified with the different types of conglomerate (Fig. 9). Cross-bed sets are typically about 50 cm thick, and commonly demonstrate normal grading and size sorting (alternate coarse and fine layers) in the foresets. Lithofacies Sp can be overlain by ripple-laminated

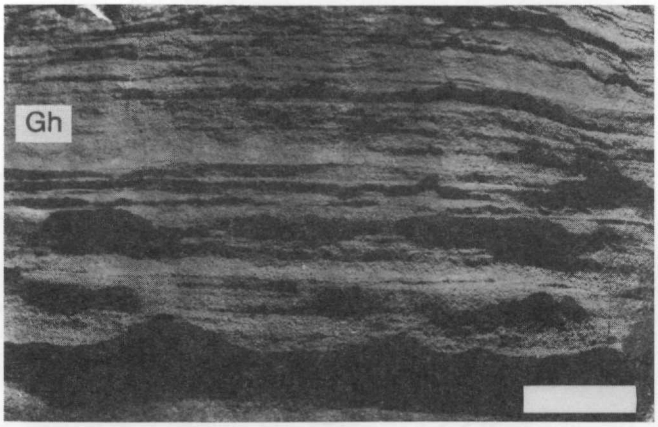

FIGURE 6. Transverse (across-stream) view of bar-tail deposits (lithofacies Gh), generally inclined at <10°. Scale bar is 15 cm.

sandstone (lithofacies Sr) or by mudstone drapes (lithofacies Fm). This type of cross bedding forms from the migration of straight-crested (transverse) dunes. Commonly, in gravel-bedload rivers, small dunes migrate through the channels between gravel bars under lower flow conditions. In some cases, flow divergence around gravel bars can be documented (for example, Evans 1991).

Sandy deposits were dominated by coarse-grained, pebbly, trough-cross-bedded sandstone (lithofacies St). These deposits were found in sets averaging 21 cm thick, and co-sets that average 100 cm thick (Fig. 10). Lithofacies St always overlies a scoured surface (lithofacies Ss) and is commonly multistory. The deposits are interpreted as three-dimensional dunes in a sand-bedload river (Collinson and Thompson 1989). In many instances, trough-cross-bedded sandstones are convoluted or recumbently folded, suggesting rapid deposition of water saturated sand that was modified by shear, possibly in response to flash-flooding conditions (Wells and others 1993).

Fine-grained deposits are very rare in the Sharon Formation. The two most common occurrences of fine-grained materials are as mudstone intraclasts (lithofacies Se) and as thin mudstone drapes above bar-platform or dune deposits (lithofacies Fm). The presence of lithofacies Se and Fm indicates that the source area for this fluvial system included fine-grained sediments. The rarity of the deposits suggests that fine-grained materials were transported through the fluvial system, but that high-energy flow conditions precluded significant accumulations (for example, Bluck 1979; Evans 1991).

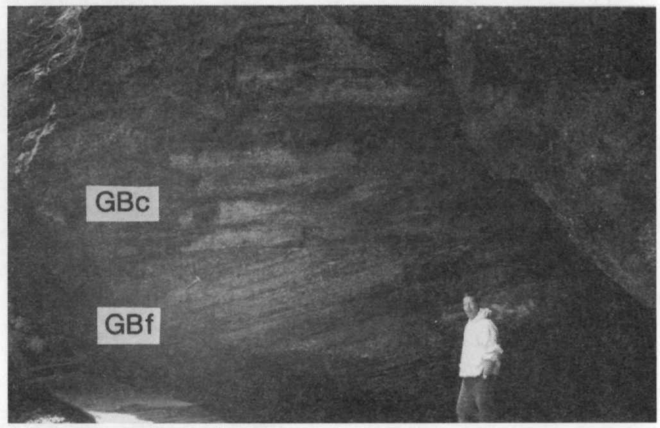

FIGURE 8. Transverse (across-stream) view of bar-margin foreset deposits (GBf) overlain by downstream progradation of bar-core (GBc) sequence. Hammer is 30 cm.

Lithofacies Assemblages

As indicated in the previous section, certain lithofacies appear to be grouped together. Markov chain analysis provides a statistical test of significance of these associations. The results are given for gravel-rich deposits (Fig. 11A) and sand-rich deposits (Fig. 11B). Statistically significant, non-random lithofacies transitions that can be identified in the gravel-rich deposits include scoured surface (lithofacies Ss) to bar platform (lithofacies Gm) and suprabar platform (lithofacies Smc) deposits, as well as the bar-margin avalanche-face deposits and adjacent sandy transverse (2-D) dune deposits. The sand-rich deposits consist of 2-D and 3-D sand dune sequences, with minor gravel bar deposits. These

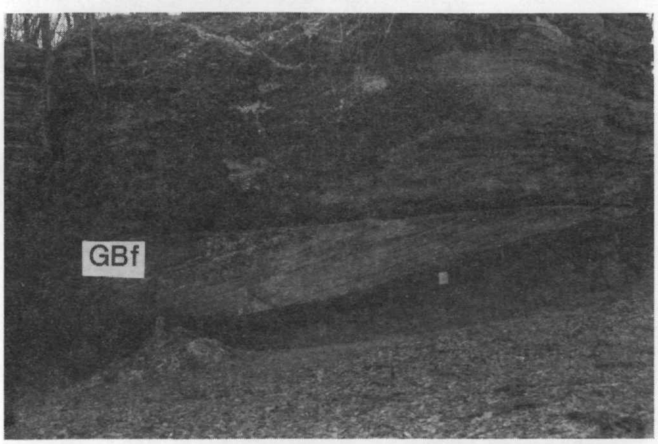

FIGURE 7. Longitudinal (downstream) view of bar-margin foreset (GBf) deposits attached to bar platform (to right), prograding downstream into adjacent pool. Post is 1.3 m tall.

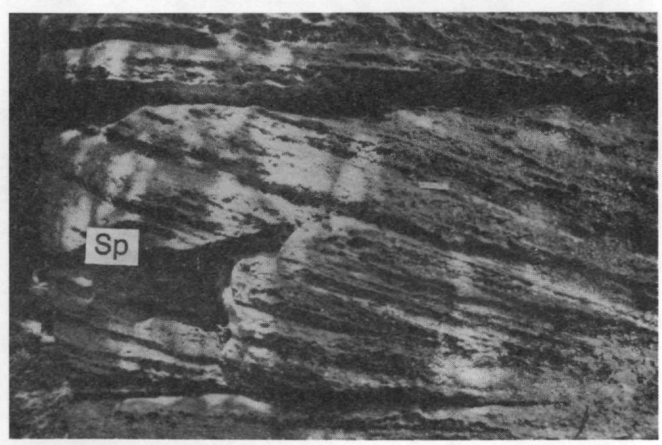

FIGURE 9. Sandy bedforms (lithofacies Sp) overlain by downstream-prograding gravel bar-tail sequence. Scale bar is 15 cm (located in center of photo).

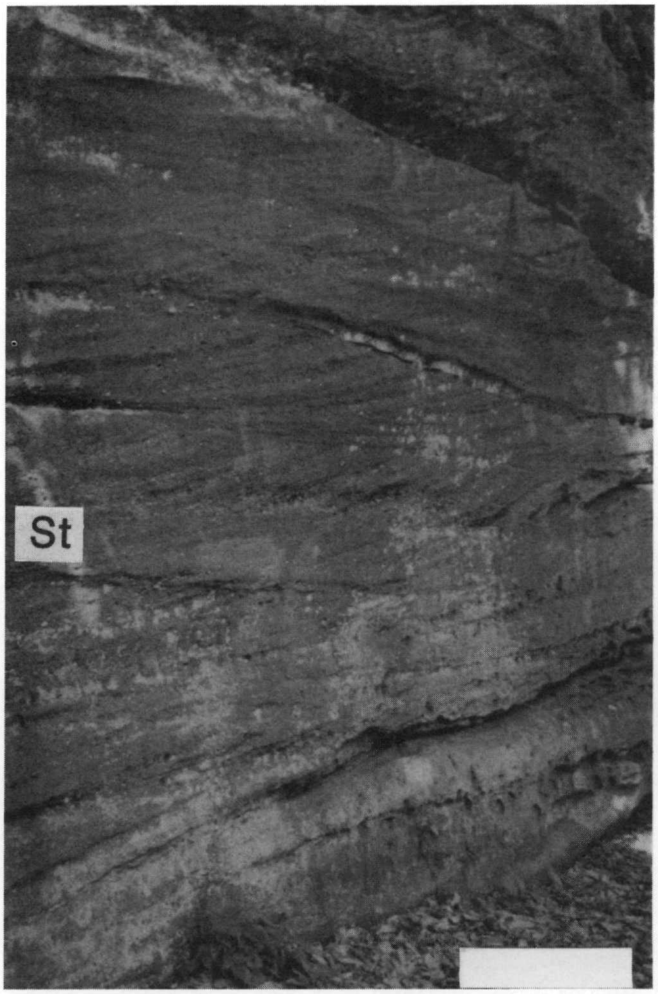

FIGURE 10. Multistory sandy bedform sequence (lithofacies St), the most common element in the sand-bedload stream deposits. Scale bar is 20 cm.

results are consistent with interpreting the Sharon Formation as gravel-bedload and sand-bedload stream deposits.

Paleohydraulic Analysis

The results from paleohydraulic studies are given in Table 3. Reconstruction of bankfull depth ranges up to 3.7 m (average about 2.1 m) in gravel-bedload streams and up to 4.5 m (average about 1.5 m) in sand-bedload streams. It is more difficult to reconstruct channel width because of fewer indicators and because erosional loss of the top of the channel deposit will have a greater effect on the width than depth. The maximum observed channel widths were 34.3 m for gravel-bedload channels and 102 m for sand-bedload channels (Fig. 12). What is more significant is that there is a relatively consistent relationship of channel depth to width, being 1:10 in gravel-bedload channels (r^2 = 0.69) and 1:40 in sand-bedload channels (r^2 = 0.89).

Paleoslopes were calculated using the methodology discussed previously. A range of values was used to account for the uncertainties of the data. The results show that paleoslopes for both gravel- and sand-bedload channels were relatively consistent in the range of 0.3 to 1.1×10^{-3} (dimensionless slope values), or 0.3 to 1.1 m/km (Table 3). These are within the low end of the range of values recorded from modern, humid-climate, fluvial systems that transport gravel (for example, Evans 1991).

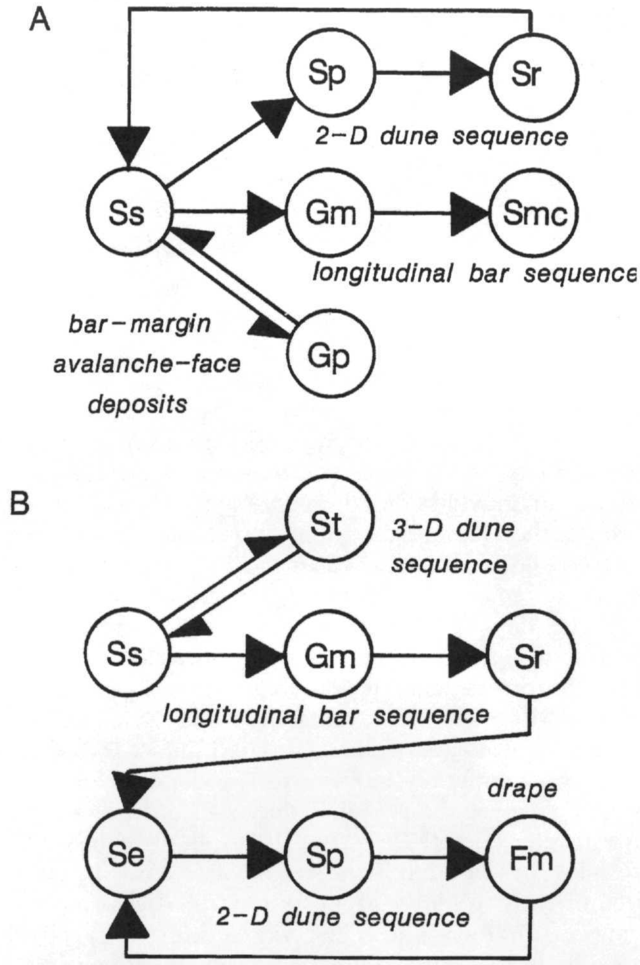

FIGURE 11. Markov chain analyses for (A) gravel-bedload stream deposits and (B) sand-bedload stream deposits in the Sharon Formation. Lithofacies codes given in Table 1.

Architectural Element Analysis

This study applied descriptions of coarse-grained stream deposits from Bluck (1979) to the method of Miall (1985). Specifically, we combined Miall's elements GB (gravel bedforms) and FM (foreset macroforms) into gravel bar-platform deposits. These were then split into bar head (GBh), bar core (GBc), bar tail (GBt), and bar margin foreset (GBf) elements (Table 2). Other important architectural elements were suprabar-platform deposits, SP (which is close to Miall's laminated sand sheets), as well as sandy bedforms (SB) and channels (CH). Each one of these elements consists of one or more lithofacies, separated from other elements by bounding surfaces.

Vertical relationships between these elements include the bar platform deposits overlain by the suprabar platform deposits, as already described. Lateral relationships include bar-head to bar-core to bar-tail, or bar-core to bar-margin, transitions already described. The use

TABLE 3

Paleohydraulic summary of the Sharon Formation.

Criterion	Sand-bedload Streams	Gravel-bedload Streams
Scour depth		
Average	0.93 m	2.12 m
Maximum	2.25 m	3.70 m
(Observations)	(14)	(8)
Height of Gravel Bar Platform		
Average	0.59 m	0.85 m
Maximum	0.85 m	1.55 m
(Observations)	(11)	(15)
Flow Depth from Dune Height		
Average	1.50 m	2.85 m
Maximum	4.50 m	3.55 m
(Observations)	(79)	(5)
Height of Bar-Margin Foresets		
Average	—	0.80
Maximum	—	1.45
(Observations)	(0)	(3)
Range of Grain Size D_{95}	1.07-3.54 cm	1.92-4.68 cm
Range of Sorting (D_{95} / D_{50})	2.14-3.01	2.13-2.74
Range of Shields Number (τ^*_{cr})	0.020-0.030	0.020-0.030
Range of Paleoslope Values	$0.2\text{-}1.2 \times 10^{-3}$	$0.3\text{-}1.1 \times 10^{-3}$

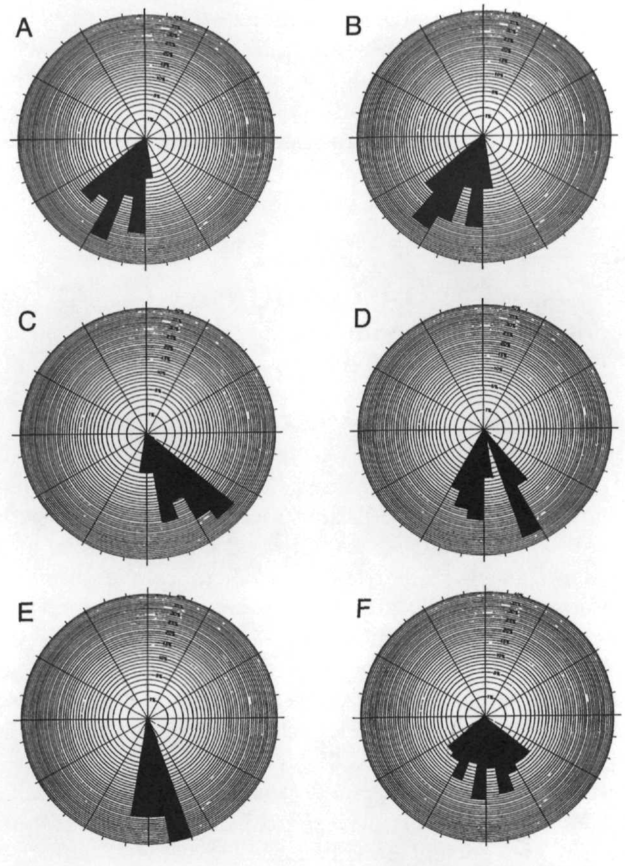

FIGURE 13. Paleocurrent data from the following locations: Whipps Ledges (A), Kendall Ledges (B), Nelson Ledges (C), Kennedy Ledges (D), and Thompson Ledges (E). A summary rose diagram is given for all locations (F). Plots are non-linear (Nemec 1988). Vector statistics given in Table 4.

of photographs in the field permits recognition of individual bars that extend as sheet-like deposits, several meters thick and 10s of meters long. The architecture confirms the lithofacies analysis completed earlier, that these deposits closely resemble those of modern braided streams (Leopold and Wolman 1957).

Paleocurrent Analysis

Paleocurrents from cross bedding data show flow was dominantly southward (Fig. 13). At any location, the low

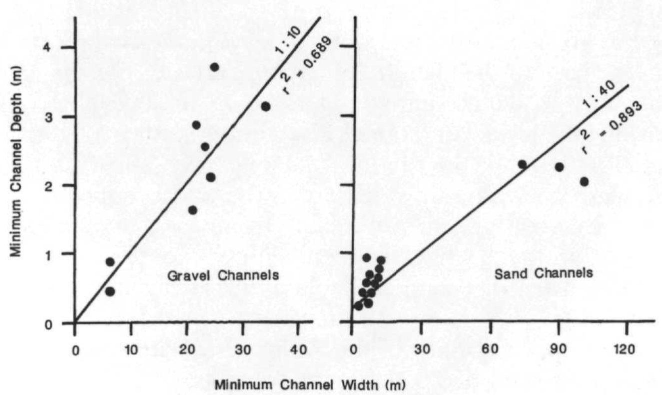

FIGURE 12. Measured paleochannel width versus depth for gravel-bedload stream deposits and sand-bedload stream deposits in the Sharon Formation.

TABLE 4

Paleocurrent data from the Sharon Formation.

Criterion	Whipps Ledges	Kendall Ledges	Nelson Ledges	Kennedy Ledges	Thompson Ledges
Number of Measurements	23	14	28	18	20
Vector Mean	201	199	148	173	172
Vector Magnitude	22.28	14.31	27.22	16.73	19.75
Circular Standard Deviation	14.29	17.35	13.50	21.51	8.98
Rayleigh's p	0.0000	0.0000	0.0000	0.0000	0.0000

Note: Paleocurrent data is from cross-bedding. Paleocurrent rose diagrams using a non-linear scale (Nemec 1988) are shown in Fig. 13. Vector mean, vector magnitude, and Rayleigh test of significance from Curray (1956). Circular standard deviation from Krause and Geijer (1987). All paleocurrent data are statistically significant (p <0.05).

dispersion of flow data is consistent with a braided stream depositional environment (Miall 1974). Data from paleochannel axes are relatively consistent with cross bedding data, although some channels diverge to the west (Ninke 1995). Our results are consistent with other studies of the Sharon Formation, indicating a northerly source area for the unit (Fuller 1955; Meckel 1967; Coogan and others 1974; Mullett and others 1990; Robinson and Prave 1995).

DISCUSSION

Depositional Environments

The Sharon Formation in northeastern Ohio is interpreted as gravel-bedload and sand-bedload stream deposits on the basis of lithofacies types, lithofacies abundances, lithofacies assemblages, depositional architecture, paleohydrology, and paleocurrent dispersion. The gravel-bedload stream deposits consist of gravel bars (lithofacies Gm, Gh, and Gp) organized into bar head, bar core, bar tail, and bar margin sequences. These bar platforms are overlain by suprabar platform deposits (lithofacies Smc and Sh) organized into laminated sand sheet sequences, and chute channels filled with small bedforms (lithofacies St and Sr). Between these gravel bars were channels that filled with sand dune deposits (lithofacies Sp). The conglomerate-sandstone-mudstone ratio for these deposits averaged 70:30:0. The characteristics of these deposits are consistent with modern and ancient gravel braided streams (Boothroyd and Ashley 1975; Church and Gilbert 1975; Miall 1977, 1978; Rust 1978, 1984; Bluck 1979; Forbes 1983; Ramos and Sopena 1983; Desloges and Church 1987).

The sand-bedload stream deposits consist predominantly of 2-D and 3-D sand dune deposits (lithofacies Sp and St). Other deposits include smaller gravel bars (lithofacies Gm and related lithofacies), mudstone intraclasts (lithofacies Se) and mudstone drapes (lithofacies Fm) in the troughs of dunes. The conglomerate-sandstone-mudstone ratio for these deposits averaged 20:78:2. The characteristics of these deposits are consistent with modern and ancient sandy braided streams (Williams and Rust 1969; Smith 1970, 1971, 1974; Cant and Walker 1978; Cant 1978; Allen 1983; Blakey and Gubitosa 1984; Lawrence and Williams 1987).

This study confirms and expands upon the braided stream interpretations of previous workers (Meckel 1967; Mrakovich and Coogan 1974; Wells and others 1993). In contrast to Coogan and others (1974) and Mrakovich (1969), we found no evidence for significant accumulations of overbank fines, lateral accretion surfaces, or point bar sequences indicative of meandering stream environments. Similarly, evidence for deltaic distributary plain or related environments is completely lacking.

Stratigraphic Trends

The Sharon Formation varies from about 15 to 80 m in thickness, due to local filling of paleovalleys up to 60 m deep, cut into the underlying Mississippian marine rocks (Winslow and White 1966; Meckel 1967; Mrakovich 1969). We believe that a composite stratigraphic section can be constructed for the Sharon Formation. The basal contact is exposed at Nelson Ledges (Ninke 1995). Previous workers have shown that two sites, Nelson Ledges and Thompson Ledges, are closely related and part of the same paleovalley fill (Coogan and others 1974). The stratigraphic sections at these two locations are similar, consisting of coarsening-upward sequence and transition from sand-bedload stream deposits to gravel-bedload stream deposits.

The sections at Kennedy Ledges, Whipps Ledges, and Kendall Ledges are also similar. Each represents sand-bedload stream deposits of approximately the same thickness (Fig. 2). The Kennedy Ledges section is less than 2.0 km from the Nelson Ledges section, and can be shown to overlie it. We suggest that the Sharon Formation shows a consistent stratigraphic trend: coarsening upward through the interval in which these fluvial systems were confined to paleovalleys, and then finer-grained through the interval in which these fluvial systems had filled and overtopped paleotopography.

Basin Evolution

Throughout the Appalachian foreland basin, an unconformity of several million years duration separates Mississippian and Pennsylvanian strata (Saunders and Ramsbottom 1986; Beuthin 1997; Driese and others 1998). This unconformity, coupled with the transition from marine shales to fluvial sandstones at the base of the Sharon Formation, suggests fall in relative base level during Late Mississippian-Early Pennsylvanian time. Evidence has been presented that such base-level fall was glacio-eustatic (Veevers and Powell 1987; Ross and Ross 1988), although it may have been accentuated in this case due to regional tectonic tilting related to migration of the peripheral bulge (Robinson and Prave 1995). Regardless of cause, the result was incision into the marine shales, and creation of paleotopography in northeastern Ohio.

Deposition of the Sharon Formation represents backfilling of paleovalleys, thus is evidence of rising base-level conditions during the Early Pennsylvanian. This interpretation is supported by evidence for glacio-eustatic sea level rise elsewhere (Veevers and Powell 1987). Tectonic subsidence is also possible, but Robinson and Prave (1995) present evidence for reduction of tectonic loading in this region during the Early Pennsylvanian. The predominance of gravelly deposits in the base of the Sharon Formation, and the coarsening-upward sequence, imply progradation under stable or rising sea level conditions. Elsewhere, studies of depositional trends in foreland basins have shown that similar coarsening-upward sequences and progradation of sheets of gravel can result from <u>loss</u> of accommodation space when sediment supply exceeds tectonic subsidence (for example, Paola 1988; Heller and Paola 1989).

The upper portion of the Sharon Formation is dominated by sand-bedload stream deposits. The transition from the underlying gravel-bedload stream deposits could be related to foreland basin tectonics (for example, changes in subsidence rates), but there is no supporting evidence for such changes. A simpler explanation is that these changes were due to the transition from fluvial systems confined to bedrock valleys to fluvial systems not confined by bedrock valleys, with concordant effects on fluvial geomorphology and sedimentology. Confined bedrock-valley fluvial systems are characterized by high magnitude flows, high flow stage, and gravel-rich deposits (for example, Baker 1984). Once paleovalleys were filled and overtopped, flow might be expected to diverge into more numerous, wider, and shallower channels. The sandy bank materials provided little bank stability, thus channel migration and switching became more pronounced, creating a wider active braidplain. Such changes can be observed today by examining the spatial changes in modern fluvial systems that exit bedrock-controlled valleys.

SUMMARY & CONCLUSIONS

This study confirms and expands upon previous interpretations of the Sharon Formation as gravel- and sand-braided stream deposits. Gravel-braided stream deposits consist of tabular gravel bar-platforms (bar-head, bar-core, bar-tail, and bar-margin deposits) commonly overlain by supra-bar platform deposits (laminated sand sheets and chute channels-fills). Between the gravel bars were sandy 2-D dune deposits. Sand-braided stream deposits consist of 2-D and 3-D dunes with minor gravel bar deposits. In contrast to previous workers, no evidence supportive of meandering streams (such as lateral-accretion surfaces, point-bar deposits, or extensive overbank deposits) were observed.

Paleohydraulic reconstructions indicate that the paleochannel depth-to-width ratio for gravel braided stream channels was 1:10 (r^2 = 0.69) and for sandy braided stream channels was 1:40 (r^2 = 0.89). Average channel depths were higher for gravel braided streams (about 2.1 m) versus sand braided streams (about 1.2 m). Finally, both systems had paleoslopes in the range of 0.3 to 1.1 m/km, which is within the range noted for modern braided fluvial systems.

Following Late Mississippian-Early Pennsylvanian glacio-eustatic sealevel fall, erosion in this region produced paleovalleys with up to 60 m relief. Backfilling of these paleovalleys by the Sharon Formation indicates rising base level during the Early Pennsylvanian, probably controlled by glacial eustasy (Veevers and Powell 1987). The progradation of gravelly braidplain deposits into northeastern Ohio (producing a coarsening-upward sequence) may suggest reduced tectonic subsidence for the Appalachian foreland basin at this time in this region, as supported by studies suggesting southward shifting of tectonic loads in the Alleghenian fold-and-thrust belt at this time (Robinson and Prave 1995). Together, these data suggest progradation of the Sharon fluvial system under conditions where sediment supply exceeded subsidence, and under stable or rising sea levels.

The upper part of the Sharon Formation indicates a significant re-organization of the Sharon fluvial system from gravel-braided streams to sandy-braided streams. Although eustasy, tectonics, and paleoclimate could account for such re-organization of fluvial systems, a simpler solution would be backfilling and overtopping of paleovalleys. The release from bedrock-controlled paleovalley flow could account for channel widening and shallowing, reduction in competence, changes in bank materials, changes in channel lateral migration rates and channel switching. Interestingly, paleohydraulic reconstructions of channel paleoslopes do not change significantly in this transition from gravel-braided streams to sandy-braided streams, again suggesting that these changes are not tectonic in origin.

ACKNOWLEDGMENTS. Suggestions from Charles F. Kahle, Sheila J. Roberts, Brian Jones, Douglas Cant, Neil Wells, and an anonymous reviewer significantly improved the manuscript. We also thank Gerald Lackey (Ohio Department of Natural Resources) for providing access to several research sites, and Larry Krissek for assistance obtaining a report.

LITERATURE CITED

Algeo TJ, Wilkinson BH. 1988. Periodicity of mesoscale Phanerozoic sedimentary cycles and the role of Milankovitch orbital modulation. J Geol 96:313-22.
Allen JRL. 1978. Studies in fluviatile sedimentation: An exploratory quantitative model for the architecture of avulsion-controlled alluvial suites. Sed Geol 21:129-47.
Allen JRL. 1983. River bedforms: Progress and problems. In: Collinson JD, Lewin J, editors. Modern and Ancient Fluvial Systems. Intern Assoc Sediment Spec Publ 6:19-33.
Allmendinger RW, Nelson KD, Potter CJ, Barazangi M, Brown LD, Oliver JE. 1987. Deep seismic reflection characteristics of the continental crust. Geology 15:304-10.
Andrews ED. 1983. Entrainment of gravel from naturally sorted riverbed material. Geol Soc Amer Bull 94:1225-31.
Andrews ED. 1984. Bed-material entrainment and hydraulic geometry of gravel-bed rivers in Colorado. Geol Soc Amer Bull 95:371-8.
Baker VR. 1984. Flood sedimentation in bedrock fluvial systems. In: Koster EH, Steel RJ, editors. Sedimentology of Gravels and Conglomerates. Can Soc Petrol Geol Mem 10:87-98.
Beuthin JD. 1997. Paleopedological evidence of eustatic Mississippian-Pennsylvanian (Mid-Carboniferous) unconformity in southern West Virginia. Southeastern Geol 37:25-7.
Blakey RC, Gubitosa R. 1984. Controls on sandstone body geometry and architecture in the Chinle Formation (Upper Triassic), Colorado Plateau. Sed Geol 38:51-86.
Bluck BJ. 1979. Structure of coarse grained braided stream alluvium. Trans Royal Soc Edinburgh 70:181-221.
Boothroyd JC, Ashley GM. 1975. Processes, bar morphology, and sedimentary structures on braided outwash fans, northeastern Gulf of Alaska. In: Jopling AV, McDonald BC, editors. Glaciofluvial and Glaciolacustrine Sedimentation. SEPM Spec Publ 23:193-222.
Bowen CH. 1953. Petrology and economic geology of the Sharon Conglomerate in Geauga and Portage Counties, Ohio. Columbus: Ohio St Univ Eng Exp Stat Bull 153:1-58.
Bridge JS, Leeder MR. 1979. A simulation model of alluvial stratigraphy. Sedimentol 26:617-44.
Brown MB. 1983. Two-way tables, empty cells, and departures from independence. In: Dixon WJ, Brown MB, editors. BMDP-83, Biomedical Computer programs, P-Series. Los Angeles: Univ of California Pr. p 278-96.
Butcher SW. 1990. The nickpoint concept and its implications regarding onlap to the stratigraphic record. In: Cross TA, editor. Quantitative Dynamic Stratigraphy. Englewood Cliffs (NJ): Prentice-Hall. p 375-85.
Butts C. 1908. The unconformity between the Mississippian and Pennsylvanian, and its bearing on questions of geologic correlation. Science 27:992-3.
Cant DJ. 1978. Development of a facies model for sandy braided river sedimentation: Comparison of the South Saskatchewan River and the Battery Point Formation. In: Miall AD, editor. Fluvial Sedimentology. Can Soc Petrol Geol Mem 5:627-39.
Cant DJ, Walker RJ. 1978. Fluvial processes and facies sequences in the sandy braided South Saskatchewan River, Canada. Sedimentol 25:625-48.

Carr TR. 1982. Log-linear models, Markov chains, and cyclic sedimentation. J Sed Petrol 52:905-12.
Cecil CB. 1990. Paleoclimate controls on stratigraphic repetition of chemical and siliciclastic rocks. Geology 18:533-6.
Cecil CB, Dulong FT. 1998. Pennsylvanian paleoclimates, sediment flux, and lithostratigraphy, Appalachian basin. Geol Soc Amer Abstr with Programs 30(2):9.
Cecil CB, Dulong FT, Edgar NT, West R. 1997. Climatic controls on Carboniferous cyclic sedimentation, U.S.A. Amer Assoc Petrol Geol, Abstract Vol 6:19.
Church M, Gilbert R. 1975. Proglacial fluvial and lacustrine environments. In: Jopling AV, McDonald BC, editors. Glaciofluvial and Glaciolacustrine Sedimentation. SEPM Spec Publ 23:22-100.
Collins HR. 1979. The Mississippian and Pennsylvanian (Carboniferous) systems in the United States—Ohio. USGS Prof Paper 1110-E:1-26.
Collinson JD, Thompson DB. 1989. Sedimentary Structures. London: Unwin and Allen. 207 p.
Coogan AH, Feldmann RM, Szmuc EJ, Mrakovich JV. 1974. Sedimentary environments of the Lower Pennsylvanian Sharon Conglomerate near Akron, Ohio. In: Heimlich RA, Feldman RM, editors. Selected Field Trips in Northeastern Ohio. Columbus: Ohio Geol Surv Guidebook 2:19-41.
Crowell JC. 1978. Gondwanan glaciation, cyclothems, continental positioning, and climate change. Am J Sci 278:1345-72.
Curray JR. 1956. The analysis of two-dimensional orientation data. J Geol 64:117-31.
Desloges JR, Church M. 1987. Channel and floodplain facies in a wandering gravel-bed river. In: Ethridge FG, Flores RM, Harvey MD, editors. Recent Developments in Fluvial Sedimentology. SEPM Spec Publ 39:99-109.
Driese SG, Caudill MR, Srinivasan K. 1998. Late Mississippian to Early Pennsylvanian paleokarst in east-central Tennessee: Field, petrographic, and stable isotope evidence. Southeastern Geol 37:189-204.
Ethridge FG, Schumm SA. 1978. Reconstructing paleochannel morphologic and flow characteristics: Methodology, limitations, and assessment. In: Miall AD, editor. Fluvial Sedimentology. Can Soc Petrol Geol Mem 5:702-21.
Evans JE. 1991. Facies relationships, alluvial architecture, and paleohydrology of a Paleogene, humid-tropical alluvial-fan system: Chumstick Formation, Washington State, U.S.A. J Sed Petrol 61:732-55.
Evans JE, Terry DO. 1994. The significance of incision and fluvial sedimentation in the basal White River group (Eocene-Oligocene), Badlands of South Dakota, U.S.A. Sed Geol 90:137-52.
Fettke CR. 1938. The Bradford Oil Field, Pennsylvania and New York. Penn Geol Surv 4th series, M21:1-454.
Forbes DL. 1983. Morphology and sedimentology of a sinuous gravel-bed channel system: lower Babbage River, Yukon coastal plain, Canada. In: Collinson JD, Lewin J, editors. Modern and Ancient Fluvial Systems. Intern Assoc Sediment Spec Publ 6:195-206.
Friend PF. 1978. Distinctive features of some ancient river systems. In: Miall AD, editor. Fluvial Sedimentology. Can Soc Petrol Geol Mem 5:531-42.
Friend PF. 1983. Towards a field classification of alluvial architecture or sequence. Modern and Ancient Fluvial Systems. In: Collinson JD, Lewin J, editors. Modern and Ancient Fluvial Systems. Intern Assoc Sediment Spec Publ 6:345-54.
Fuller JO. 1955. Source of the Sharon Conglomerate of northeastern Ohio. Geol Soc Am Bull 66:59-176.
Gastaldo RA, Dimichele WA, Pfefferkorn HW. 1996. Out of the icehouse and into the greenhouse: A Late Paleozoic analog for modern global vegetational change. GSA Today 6:1-7.
Harper CW. 1984. Improved methods of facies sequence analysis. In: Walker RG, editor. Facies Analysis. Geosci Can Reprint Ser 1:11-3.
Hatcher RD. 1972. Developmental model for the southern Appalachians. Geol Soc Am Bull 83:1735-60.
Heller PL, Paola C. 1989. The paradox of Lower Cretaceous gravels and the initiation of thrusting in the Sevier orogenic belt, United States Western Interior. Geol Soc Am Bull 101:864-75.
Krause RGF, Geijer TAM. 1987. An improved method for calculating the standard deviation and variance of paleocurrent data. J Sed Petrol 57:779-80.
Krissek LA, Ketring CL Jr, Kulikowski DL. 1986. Lower Pennsylvanian sandstones of southeastern Ohio: Implications for sediment sources and depositional environments in the north-central Appalachian basin. In: Shumaker RC, editor. Appalachian Basin Industrial Associates, Program for Fall Meeting, 1986 October 16-17. Vol 11. p 109-41.
Lamb GF. 1911. The Mississippian-Pennsylvanian unconformity and the Sharon Conglomerate. J Geol 19:104-9.
Lawrence DA, Williams BPJ. 1987. Evolution of drainage systems in response to Acadian deformation: The Devonian Battery Point Formation, Eastern Canada. In: Ethridge FG, Flores RM, Harvey MD, editors. Recent Developments in Fluvial Sedimentology. SEPM Spec Publ 39:287-300.
Leopold LB, Wolman MG. 1957. River channel patterns: Straight, braided, and meandering. USGS Prof Paper 232-B:39-85.
Maizels JK. 1983. Paleovelocity and paleodischarge determination for coarse gravel deposits. In: Gregory KJ, editor. Background to Paleohydrology. London: Wiley Interscience. p 101-39.
Meckel LD. 1967. Origins of Pottsville conglomerates (Pennsylvanian) in the central Appalachians. Geol Soc Am Bull 78:223-58.
Miall AD. 1974. Paleocurrent analysis of alluvial sediments: A discussion of directional variance and vector magnitude. J Sed Petrol 44:1174-85.
Miall AD. 1977. A review of the braided river depositional environment. Earth Sci Rev 13:1-62.
Miall AD, editor. 1978. Lithofacies types and vertical profile models in braided river deposits: A summary. Fluvial Sedimentology. Can Soc Petrol Geol Mem 5:597-604.
Miall AD. 1985. Architectural-element analysis: A new method of facies analysis applied to fluvial deposits. Earth Sci Rev 22:261-308.
Miall AD. 1993. The architecture of fluvial-deltaic sequences in the Upper Mesaverde Group (Upper Cretaceous), Book Cliffs, Utah. In: Best JL, Bristow CS, editors. Braided Rivers. Geol Soc London Spec Publ 75:305-32.
Miall AD. 1994. Reconstructing fluvial macroform architecture from two-dimensional outcrops: Examples from the Castlegate Sandstone, Book Cliffs, Utah. J Sed Res B64:146-58.
Miller DJ, Eriksson KA. 1999. Linked sequence development and global climate change: The Upper Mississippian record in the Appalachian basin. Geology 27:35-8.
Mohrig DC. 1987. Facies and paleohydrology of a floodplain-dominated braided fluvial system: Cretaceous Ventura redbeds, Washington, U.S.A. Seattle: Univ of Washington. Unpubl MSc thesis. 37 p.
Mohrig DC, Smith JD. 1991. Measured distributions of river dunes and implications to construction of stratification. Geol Soc Am Abstr with Programs 23(6):A462.
Mrakovich JV. 1969. The Sharon Conglomerates of northeastern Ohio. The Compass 46:150-8.
Mrakovich JV, Coogan AH. 1974. Depositional environment of the Sharon Conglomerate Member of the Pottsville Formation in northeastern Ohio. J Sed Petrol 44(4):1186-99.
Mullett DJ, Kurlich RA, Frech KR, Wells NA. 1990. Paleocurrent analysis of the Sharon Conglomerate and sandstone lithosomes in the vicinity of Ice Box Cave at Kendall Ledges Park, Summit County, Ohio. The Compass 68(1):21-32.
Nadon GC. 1998. An allostratigraphic approach to the Pennsylvanian sediments of Athens County, southeastern Ohio. Geol Soc America Abstr with Programs 30(2):63.
Nemec W. 1988. The shape of the rose. Sed Geol 59:149-52.
Ninke DJ. 1995. Using facies relationships, alluvial architectural-element analysis, and paleohydraulic reconstructions to determine evolutionary changes in the Sharon depositional basin. Bowling Green (OH): Bowling Green State Univ. Unpubl MSc thesis. 84 p.
Paola C. 1988. Subsidence and gravel transport in alluvial basins. In: Kleinspehn KL, Paola C, editors. New Perspectives in Basin Analysis. New York: Springer-Verlag. p 231-43.
Phillips TL, Peppers RA. 1984. Changing patterns of Pennsylvanian coal-swamp vegetation and implications of climatic control on coal subsidence. Intern J Coal Geol 3:205-55.
Powers DW, Easterling RG. 1982. Improved methodology for using embedded Markov chains to describe cyclical sediments. J Sed Petrol 52:913-23.
Ramos A, Sopena A. 1983. Gravel bars in low-sinuosity streams (Permian and Triassic, central Spain). In: Collinson JD, Lewin J, editors. Modern and Ancient Fluvial Systems. Intern Assoc Sedimentol Spec Publ 6:301-12.
Robinson AJ, Prave AR. 1995. Cratonal contributions to a classic molasse: The Carboniferous Pottsville Formation of eastern Pennsylvania revisited. Geology 23:369-72.
Ross CA, Ross JRP. 1985. Late Paleozoic depositional sequences are synchronous and worldwide. Geology 13:194-7.

Ross CA, Ross JRP. 1988. Late Paleozoic transgressive-regressive deposition. In: Wilgus CK, Hastings BS, Kendall CGSC, Posamentier HW, Ross CA, Wagoner JC, editors. Sea Level Changes—An Integrated Approach. SEPM Spec Publ 42:227-48.

Rust BR. 1978. Depositional models for braided alluvium. In: Miall AD, editor. Fluvial Sedimentology. Can Soc Petrol Geol Memoir 5:605-25.

Rust BR. 1984. Proximal braidplain deposits in the Middle Devonian Malbaie Formation of Eastern Gaspe, Quebec, Canada. Sediment 31:675-95.

Saunders WB, Ramsbottom WHC. 1986. The mid-Carboniferous eustatic event. Geology 14:208-12.

Slingerland RL, Beaumont C. 1989. Tectonics and sedimentation of the upper Paleozoic foreland basin in the central Appalachians. In: Sedimentology and Thermal-mechanical History of basins in the Central Appalachian Orogeny. International Geological Congress, 28th, Washington, DC. Field trip Guidebook T152:4-24.

Smith ND. 1970. The braided stream depositional environment: Comparison of the Platte River with some Silurian clastic rocks, north-central Appalachians. Geol Soc Am Bull 81:2993-3014.

Smith ND. 1971. Transverse bars and braiding in the Lower Platt River, Nebraska. Geol Soc Am Bull 82:3407-20.

Smith ND. 1974. Sedimentology and bar formation in the upper Kicking Horse River, a braided outwash stream. J Geol 82:205-23.

Stout W. 1916. Geology of Muskingham County. Ohio Geol Surv Bull 21, 4th Ser. 351 p.

Turk G. 1979. Transition analysis of structural sequences: Discussion and reply. Geol Soc Am Bull 90:989-91.

Veevers JJ, Powell CM. 1987. Late Paleozoic glacial episodes in Gondwanaland reflected in transgressive-regressive depositional sequences in Euramerica. Geol Soc Am Bull 98:475-87.

Wanless HR, Shepard FP. 1936. Sea level and climatic changes related to Late Paleozoic cycles. Geol Soc Am Bull 47:1177-206.

Wells NA. 1999. ASTRA.BAS: A program in QuickBasic 4.5 for exploring rose diagrams, circular histograms, and some alternatives. Computers & Geosciences 25:641-54.

Wells NA, Richards SS, Peng S, Keattch SE, Hudson JA, Copsey CJ. 1993. Fluvial processes and recumbently folded crossbeds in the Pennsylvanian Sharon Conglomerate in Summit County, Ohio, USA. Sed Geol, 85:63-83.

Wiberg PL, Smith JD. 1987. Calculations of the critical shear stress for motion of uniform and heterogeneous sediments. Water Resources Res 23:1471-80.

Williams PF, Rust BR. 1969. The sedimentology of a braided river. J Sed Petrol 39:649-79.

Winslow JD, White GW. 1966. Geology and groundwater resources of Portage County, Ohio. USGS Prof Paper 511:1-80.

Zeuner FE. 1959. The Pleistocene Period: Its Climate, Chronology, and Faunal Succession. London: Hutchinson and Co. 447 p.